

Laser-based multichannel fiber optic sensor for multipoint detection of corrosion

RAZIEH SHAHPIR, SAEED GHAVAMI SABOURI, ALIREZA KHORSANDI*

Department of Physics, University of Isfahan, 81746-73441 Isfahan, I.R. Iran

*Corresponding author: a.khorsandi@phys.ui.ac.ir

We report on a multichannel sensor for multipoint corrosion monitoring of an aluminum film, which was corroded by nitric acid as a corrosive solution. The sensor head was a commercial 1×4 optical fiber coupler combined with the optical time domain reflectometry technique. The effects of the concentration and pH of acid on the corrosion rate of the aluminum film are initially studied and characterized. Then, about 100 nm of pure aluminum is coated on the end facets of each fiber channel and reduction of the back reflected signals is simultaneously monitored as a measure of corrosion rate. It is found that the fabricated sensor is very sensitive to the variation of pH as by increasing of the pH up to ~13, the corrosion rate of aluminum is raised to ~75 millimeter per year. Our experimental results have been verified by the standard immersion test, indicating very good consistency and reliability. Eventually, the sensor is used to trace the corrosion of sea water provided from the Persian Gulf, confirming the validity of laboratory results.

Keywords: optical time domain reflectometry (OTDR), multichannel corrosion, optical fiber.

1. Introduction

In recent years much effort has been directed toward developing non-destructive, *in situ* and cost-effective techniques to provide an early indication of corrosion not only for reducing the cost but also for safety and immunity [1–3]. Yet many corrosion tests are made every year in the industrial plants such as shipping, oil fields, aircraft and geotechnical structures including bridges and pipelines to evaluate their efficiency and lifetime using early-warning systems. Under special conditions, corrosion can be formed to some degree through the chemical reaction of most of the materials with corrosive environments like mineral acids, moist air, alkalis and petroleum oil. However, primary factors, including alkalinity and pH can also influence the corrosion and, therefore, on-line pH monitoring is an important issue of increasing the reliability of large structures [4–6]. Recent corrosion detection techniques provide local changes, which normally occurred after significant damage, especially in inaccessible large

areas that are operating under harsh circumstances. Thus, there is a great demand for developing of a distributed detection system for on-line and *in situ* monitoring of structural changes [7, 8]. Optical fiber distributed sensors are mostly based upon stimulated Brillouin scattering [9–11], which offers the ability of measuring macroscopic parameters such as strain and temperature over lengths of the order of thousands kilometers. A distributed sensor is capable of supporting many instruments within the optical bandwidth of a fiber for the identification and characterization of crucial problems like health monitoring of civil infrastructural systems [6, 12] and/or corrosion rate inspections in a relatively large scales [13]. In this framework, laser-coupled optical fibers show promise for the fabrication of distributed sensors because they are benefited from several advantages such as high sensitivity, immunity to electromagnetic interfaces, security and compactness [14–16]. In the realization of a fiber-based sensor, one example is the transmitting of a green laser beam over a coiled unclad multimode and step-index silica fiber to detect the corrosion rate of a Fe-C film coated symmetrically around its core [17]. The main drawback faced by a transmission-type sensor is the need to have a physical access to the both ends. In contrast, a reflection-type is very simple to install and it is very flexible and sensitive. So far, various types of reflection-based optical fiber sensors for corrosion monitoring have been designed and fabricated [18]. Distributed sensing along with sufficient resolution is typically obtained using the Rayleigh backscattered light of a launched optical pulse into an optical fiber. It is based on optical time domain reflectometry (OTDR) where it was first developed to locate the fiber defects in the communication links [15, 16]. An amplified fiber optic sensor using OTDR technique is recently demonstrated for multipoint and self-referenced monitoring of corrosion rate over a long link [19]. For sensing the corrosion process in aluminum, OTDR technique is also used to detect the light that is reflected by several sensor heads through multifiber couplers [20]. The OTDR-based distributed fiber sensors for pH measurement are represented to provide a compact and simultaneous detection of multicomponent fluorescent chemical analysis [21]. In this paper, a commercial 1×4 optical fiber coupler as sensing channels is spliced to an OTDR instrument to arrange an experimental scheme for multichannel and self-referenced corrosion sensing of the pure aluminum that is coated on the cleaved ends of fiber channels. The sensor is fabricated in two configurations. In the first design, the sensing area is increased by embedding all channel probes in a corrosive solution very close to each other. In the second arrangement, each channel probe is immersed in different solutions to achieve simultaneous detection of corrosion. In order to verify the performance and sensitivity of the fabricated sensor, the effect of pH on the corrosion of aluminum films is investigated through changing the pH of a corrosive solution. The susceptibility and reliability of two configured sensors in corrosion detection and rate have been verified with the standard weight loss test. It is found that the optical response of the first sensor scheme is very advantageous for the multipoint corrosion detection in a wide area while the second sensor can be considered for simultaneous detection of several corrosive

environments. The performance of the fabricated multichannel sensor is finally demonstrated using the detection of the aluminum corrosion in a sample of sea water provided from the Persian Gulf. Obtained results illustrate a very promising sensor for *in situ* and on-line field measurements.

2. Fabricated multichannel sensor

The fabricated sensor is schematically shown in Fig. 1. It consists of an OTDR apparatus including a light source provided by a commercial continuous-wave diode laser (Thorlabs, L850P100) operating at 850 nm with an output power of ~ 100 mW. An electronic device is used to switch the injection current of the utilized diode and hence making the laser output pulse lengths of ~ 80 ns. The laser pulses are imaged into a 1.2-km multimode fiber and after passing through a polarized beam splitter (BS) the back reflected pulses are then resolved using a PIN detector (Thorlabs, PDA100A) connected to a 2-GHz bandwidth oscilloscope (Tektronix 2024B). The described OTDR system is then spliced to a multichannel sensor element, which consisted of

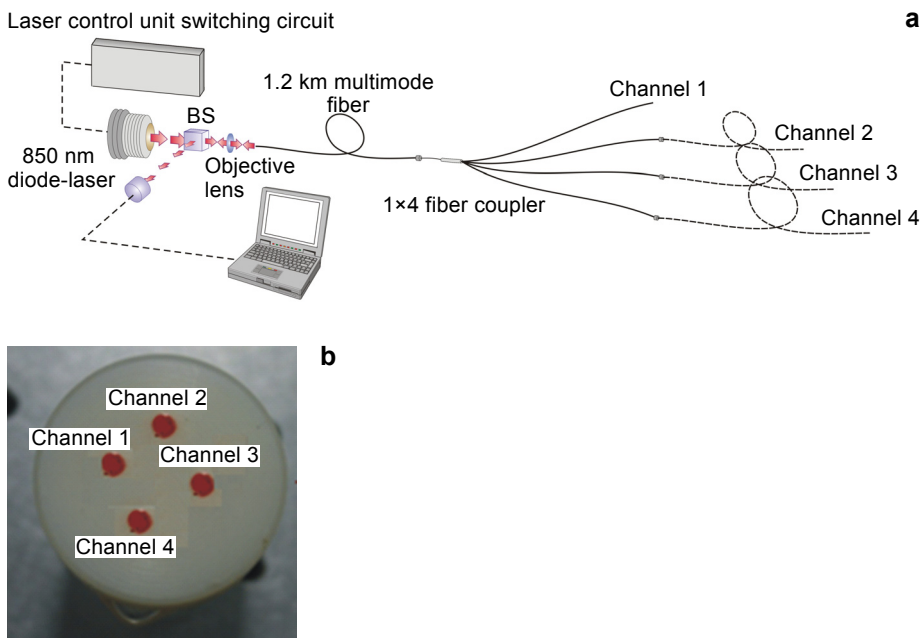


Fig. 1. The schematic of OTDR-based multichannel sensor fabricated for multipoint and simultaneous detection of corrosion; each channel appropriating equal fraction of launched power (a). Sensor head of the first sensor configuration fabricated from Teflon used for corrosion rate (CR) measurement of the aluminum film coated on the end facets of the channel probes using concentration-variable nitric acid as corrosive solution; on the head, holes with a diameter of one millimeter and one centimeter apart from each other are made; the whole sensing area is ~ 0.05 mm² and the size of sensing probe is $\sim 10 \times 10$ cm² (b).

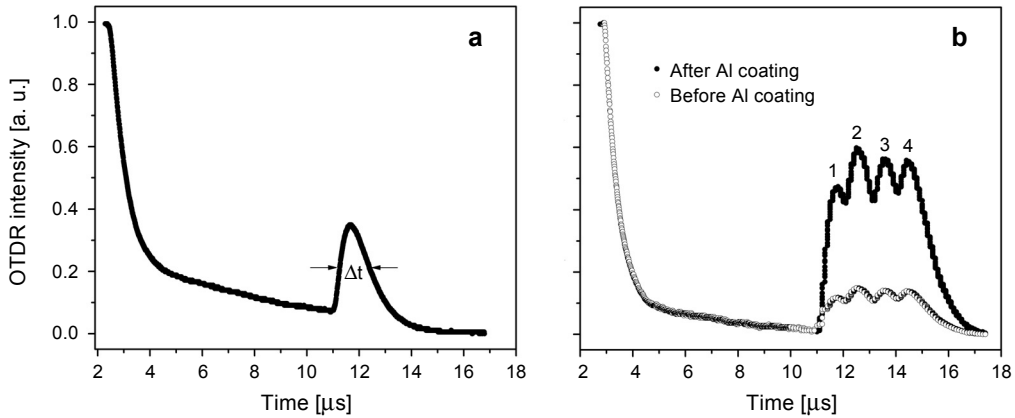


Fig. 2. Trace of the OTDR signal detected from four channels of the utilized 1×4 coupler spliced to the 1.2-km multimode fiber. The width of the traced signal is measured $0.9\ \mu\text{s}$ (a). OTDR trace of the back reflected pulses before and after coating the four probe heads with $\sim 100\ \text{nm}$ aluminum film (b). The thickness of coated layer is nearly the same for all channels and the observed intensity difference between the probes is due to the splicing losses induced by the intermediate fibers.

a commercial 1×4 multimode optical fiber coupler (OEmarket, MMC-850- 1×4 -62.5N) with a mean insertion loss of $\sim 5.5\ \text{dB}$. The length of each channel probe is one meter. The coupler was so fabricated by the manufacturer that the fraction of power carried by each channel is equal. On the sensor head, four holes with a diameter of one millimeter and one centimeter apart from each other were devised to held four fiber channels.

Figure 2 shows the traced OTDR signal reflected back from the channel heads. As evident from Fig. 2a, the peaks of the reflected signals backing from the coupler ends are beyond the OTDR dynamic range and thus cannot be separately resolved. This is due to the limitation constrained by the measured width of the OTDR signal, which imposes a resolution length of $\sim 100\ \text{m}$ on the system. Therefore, to increase the described resolution and hence avoiding the overlap between the pulses reflected from the channel ends, we increased the length of each channel probe by splicing 100, 200 and 300 m of a silica-based commercial multimode fiber having the same material as the coupler, as intermediate connection to the channels 2, 3 and 4, respectively. Accordingly, by using the standard thermal evaporation, the end facet of each channel probe is coated with $\sim 100 \pm 1\ \text{nm}$ of 99.99% pure aluminum film by a coating rate of $\sim 1\ \text{Å}/\text{sec}$ inside a vacuum chamber kept at $\sim 10^{-6}$ torr. Such fabricated sensor element was used for the corrosion monitoring of the coated films in a provided concentration-variable nitric acid as a corrosive solution. Figure 2b shows the trace of back reflected pulses before and after coating the multichannel sensor heads. As can be seen by using the intermediate fibers, the traced signals of the four channel probes are resolvable and their sensitivity to the back reflected signal is quite appreciable.

3. Sensing principles and measurement results

Corrosion monitoring is based on the reduction of back reflected pulses at the input while the aluminum layer deposited on the end facets is corroded by a corrosive solution with a certain rate of [22]

$$CR = \frac{\Delta L}{\Delta t} \quad (1)$$

where CR – corrosion rate, ΔL – the thickness reduction of the coated layer during the measurement time Δt . Aluminum is one of the most frequently used metal in industrial structures, which shows very good resistance to corrosion due to the formation of a very thin oxide layer on its surface in connection with moisture and air [23]. It is observed that depending on the pH level, the CR of the aluminum can be increased in either acid or base environments [23]. On the other hand, the effect of dilute nitric acid with the concentration below 80% on the aluminum corrosion is experimentally observed and reported [23, 24]. Therefore, to investigate the response characteristics of the fabricated sensor and hence CR measurement of the coated aluminum film, the experiment is performed for different concentrations of nitric acid of 25%, 45% and 65% for two sensor configurations.

3.1. The CR measurement using first sensor configuration

The aim of using the first sensor configuration is to increase the surface area of the detection zone by a factor of 4, from $\sim 0.012 \text{ mm}^2$ for a single fiber to $\sim 0.05 \text{ mm}^2$ for the multichannel probe. By a designed noncorrosive holder shown in Fig. 1 each

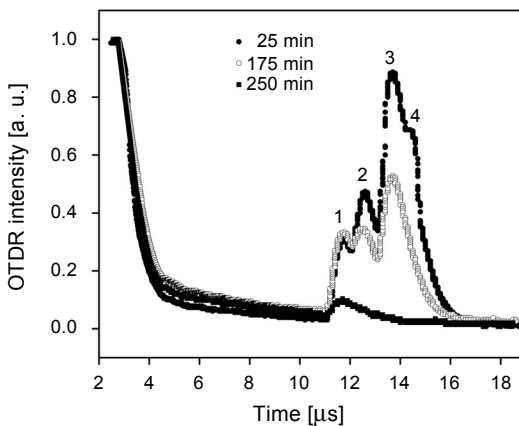


Fig. 3. Reduction of the back reflected signals from a four channel head in three time intervals while contacting with acid. The measurement is started with a nitric acid solution of 45% and the aluminum layer thickness of $\sim 100 \text{ nm}$ coated on the end facets of each channel.

channel head was then capable of monitoring the CR within the provided sensing area. The explained sensor head is inserted into the provided solutions and the reduction of the OTDR reflected signals backing from probes 1 to 4 are simultaneously monitored for three different concentrations of nitric acid. The data acquisition is performed every 5 minutes. Figure 3 indicates the variation of the OTDR signals received from four channel probes in three distinct times while the sensor head is placed in the nitric acid of 45% concentration.

As can be seen (because of the corrosion and reduction of the Al thickness), the OTDR signals of the four channels are significantly decreased and descended to $\sim 50\%$ of their initial intensity after about 175 minutes, which are in contact with the corrosive solution. However, by increasing the time, 4th peak has gradually disappeared because the low-intensity OTDR signal is passing through a pre-spliced lossy 300-m-long silica fiber. Moreover, after a certain time for each channel, the aluminum corrosion is approximately stopped and the OTDR intensities are tending to a relatively constant value. The same trend is also observed in using other nitric acid concentrations. Figure 4 shows the variation of the OTDR peaks with time for four channel probes while the aluminum-coated sensor head is placed into the provided nitric acid solution of 45%.

It is clearly shown that as long as the corrosion takes place, the OTDR signals strongly drop and tend to a minimum value. Final results of CR measurement are summarized in Table 1.

The same results as listed in Table 1 have been obtained using nitric acid with 25% and 65% of concentrations. Subsequently, as shown in Fig. 5, the variation of the mean corrosion rate can be plotted with the concentration of corrosive solution. As can be seen in Fig. 5, by increasing the acid concentration from 25% to 65%, CR has decreased from 11 to 8 of mean mpy (mpy – millimeter per year) with the measured slope of

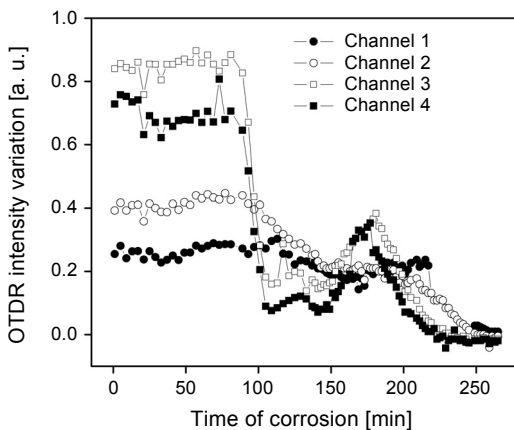


Fig. 4. Variation of the OTDR signals detected from channels 1 to 4 while the sensor head is left into a 45% concentration of nitric acid for ~ 275 min. The point of each curve corresponds to the collected data of intensity variation acquired every 5 min for each channel. The intensity of the channels is decreasing by the same order as that in Fig. 3.

Table 1. Case example of corrosion measurement reported for the nitric acid of 45% concentration. About 100 nm aluminum film is deposited on the end facets of four channel probes while the sensor head is placed in the corrosive solution. Similar results were obtained for 25% and 65% acid.

Channel probe	Corrosion time [min]	Corrosion rate (CR)	
		[nm/min]	[mpy]*
1	243	0.412 ± 0.004	9 ± 0.08
2	251	0.399 ± 0.004	8 ± 0.08
3	225	0.445 ± 0.004	9 ± 0.08
4	215	0.466 ± 0.004	10 ± 0.08
Mean corrosion rate		0.430 ± 0.004	9 ± 0.08

* mpy – millimeter per year

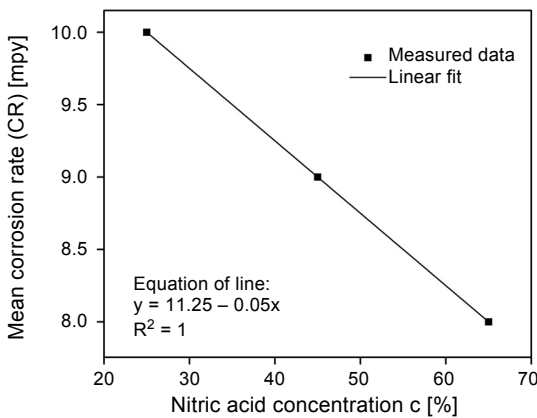


Fig. 5. Variation of mean corrosion rate with nitric acid concentration using the obtained results is listed in Table 1. Similar results are obtained like those listed in Table 1 for two other concentrations. Each point in the figure corresponds to the average of CR over four channels.

-0.05 mpy/c. Therefore, in the case of using high concentration solutions, the lengthening of corrosion procedure is possible, resulting in the safety and longevity of hazardous structures.

3.2. The CR measurement using second sensor configuration

In this part of measurement, channel probes 1, 2 and 3 are separately inserted into the provided 25%, 45% and 65% concentrations of nitric acid, respectively. This enabled the simultaneous detection of the corrosion of aluminum films that are coated on the head probes. By the same procedure and similar experimental conditions as used in corrosion measurement with the first sensor configuration, the reduction of received OTDR peaks reflected from each channel probe is monitored every 5 minutes. The trend of corrosion is illustrated in Fig. 6.

As can be seen from the plot, a feature of OTDR signal variation is principally similar to the curves indicated in Fig. 5 with a difference that the drop of OTDR signal

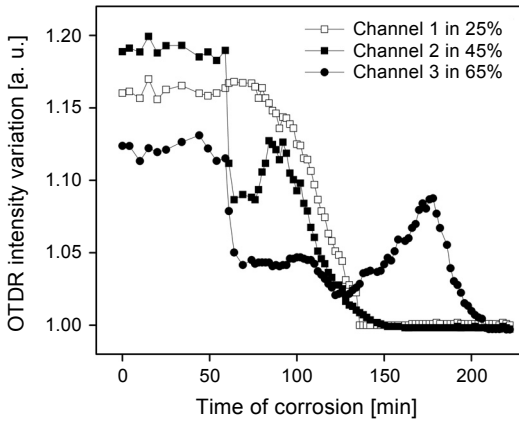


Fig. 6. Variation of the OTDR signals with time detected from channel 1, 2 and 3 while the probes have been left into the 25%, 45% and 65% concentrations of nitric acid, respectively, for ~275 minutes. Each point of the curves is related to the intensity variation of each probe that is monitored every 5 minutes. Experimental conditions are the same as used in plotting Fig. 4 and the aluminum film is initially ~100 nm.

Table 2. Summarized results of simultaneous measurement of ~100 nm aluminum film corrosion, which was initially deposited on the end facets of channel probes 1, 2 and 3 while placed in 25%, 45% and 65% of nitric acid, respectively.

Channel probe	Corrosion time [min]	Corrosion rate (CR)	
		[nm/min]	[mpy]
1	138	0.725 ± 0.008	15 ± 0.15
2	152	0.659 ± 0.008	13 ± 0.15
3	210	0.477 ± 0.008	10 ± 0.15

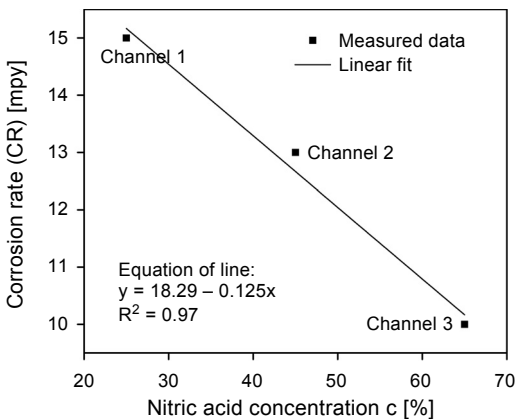


Fig. 7. Variation of CR while channels 1, 2 and 3 of corrosion sensor are individually left in the nitric acid with 25%, 45% and 65% of concentration, respectively. The thickness of aluminum film coated on the end facets of channels is initially ~100 nm.

is strongly descending for dilute nitric acids. In Table 2 the results of this measurement are summarized and the results are graphically gathered in Fig. 7.

As it is evident from the above plot, compared to the measurement obtained with the first sensor configuration, aluminum film is corroded with a larger slope of -0.125 mpy/c, indicating higher sensitivity to different environment containing different levels of corrosion. The obtained results indicate that by this configuration, multipoint corrosion monitoring is possible at the same time. Therefore, it can be used to replace multisensor devices with effective reduction in cost and size.

4. Verification of measurement using an immersion test

To verify the trend of experimental results we employed the immersion standard test basing on the same conditions as those used in the foregoing sections with equal volume of nitric acid. It is based on the weight loss ΔW measurement of a corroded sample in a relatively long and adequate time. Accordingly, CR can be evaluated using the following relation as [4]

$$CR = \frac{\Delta W}{\rho A t} \times 5.34 \times 10^5 \quad (2)$$

where ρ [g/cm^3] is the sample density, A [cm^2] is the sample surface contacting with the corrosive solution and t [h] is the time of immersion. Thus, an aluminum sample with the same purity as used for the Al deposition is provided in three similar pieces with 1 cm in width, 3 cm in length and 1 mm in diameter. The weight measurement of the provided samples is performed using a very precise balance with an accuracy of ± 0.001 gram. A 20 cm^3 volume of the utilized acids of 25%, 45% and 65% concentrations is provided and the CR is measured after immersing the aluminum pieces inside the solutions for about one week. It is performed through the weight loss measurement

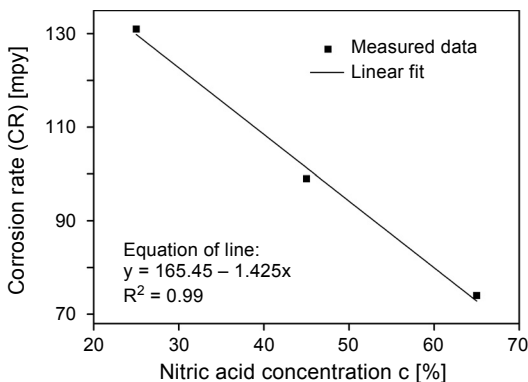


Fig. 8. Immersion test results of the aluminum corrosion to verify the measured CR performed with the multichannel sensor described in Figs. 5 and 7. The initial weight of aluminum pieces is ~ 0.251 g and the final are 0.199, 0.211 and 0.220 g for 25%, 45% and 65% of nitric acid concentrations, respectively, after ~ 7 days. The aluminum density is assumed 2.7 g/cm^3 .

of the immersed pieces and simultaneous use of Eq. (2). The results of this measurement are depicted in Fig. 8.

It is evident from the plot that the same reduction trend can be observed as that obtained with the fabricated multichannel sensor. However, the difference between the measured and evaluated CR is due to the fact that the effective surface of corrosion in the immersion test is much larger than that of the surface head of the multichannel sensor.

5. The effects of pH on the corrosion rate

Further investigation is also based on the effect of pH on aluminum corrosion. The pH of the corrosive solution is accordingly changed in a relatively wide range from zero to ~13. This was performed by adding a certain volume of distilled water into nitric acid and sodium hydroxide (NaOH) to provide acid and base environments, respectively. The pH of the compositions is measured using a standard turnsole paper. The CR measurement is then accomplished twice using the multichannel sensor in the second configuration where the end facets of channel probes 1, 2 and 3 have been coated and placed into the corrosive solutions of different pH values. Quantitative measurement is performed every 2 minutes by the monitoring of OTDR signal reduction of the utilized channels. Figure 9 illustrates the measured CR of the deposited aluminum *versus* pH of corrosive solutions.

As can be seen, the sensor appears to be quite sensitive to the pH of corrosive solution. While the pH is increased up to ~13, the CR is jumped to ~75 mpy, which indicates a very consistent feature as reported in the relevant literature [23]. Finally, the performance of the fabricated sensor is demonstrated through field measurement of CR using provided water from Persian Gulf. The combination of extreme heat and high humidity

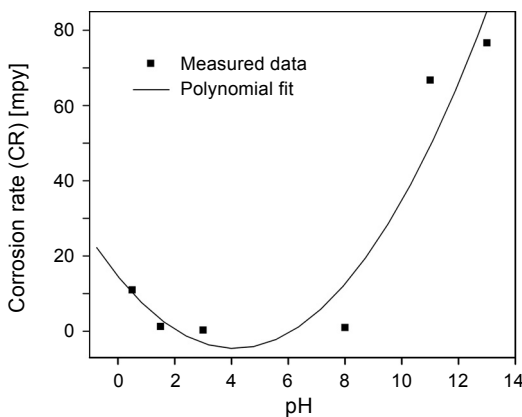


Fig. 9. Measured CR *versus* pH of corrosive solutions. A variation of the pH is performed using nitric acid and sodium hydroxide (NaOH) to make acid and base solutions. The channel probes 1, 2 and 3 of the multichannel sensor are used for simultaneous monitoring of OTDR signal reduction, which is received from the utilized channels. The thickness of the coated aluminum is initially set for ~100 nm.

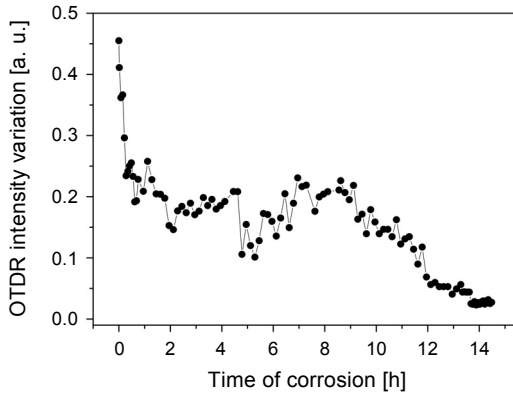


Fig. 10. Measurement of the CR of aluminum film corroded in the provided water from Persian Gulf. The sensor head is also coated with ~ 100 nm of pure aluminum and then it is left in the water for ~ 15 h.

make the Persian Gulf as one of the most aggressive environments in the world. Inside the water, chloride ion acts as a corrosion agent, which imposes very undesirable conditions on the durability of marine and submarine structures, which in turn reduces the service lifetime, and affects the regional economy. Therefore, we used a single-channel of the fabricated sensor to evaluate its performance in a real scale. The results of this measurement are depicted in Fig. 10.

As can be seen, the OTDR-based sensor appears to be quite reliable where the same CR feature can be observed as to the results obtained in the laboratory scale. However, a CR of ~ 3 mpy is obtained in this measurement.

6. Conclusion

In this work, we introduced an OTDR-based multichannel sensor for the CR monitoring of aluminum in nitric acid as a corrosive solution. It consists of an OTDR device that is spliced to a commercial 1×4 optical fiber coupler as the sensing element. To increase the resolution of a signal, the length of channel probes is increased by splicing 100, 200 and 300 m of silicon-based optical fibers to the channels 2, 3 and 4, respectively. The sensor is then used in two different configurations to provide surface and simultaneous detection of CR of aluminum film in corrosive environments. It is performed by coating the end facets of channel heads with ~ 100 nm of pure aluminum, which was placed in nitric acid solutions with three different concentrations of 25%, 45% and 65%. The CR measurement is performed by systematic detection of the OTDR signal reduction while the probe heads were placed into the corrosion solutions. By the first sensor configuration, CR detection of the surface was then possible, indicating a slope of -0.05 mpy/c while the nitric acid concentration changed from 25% to 65%. Whereas the second sensor configuration fabricated for simultaneous detection of corrosion indicated a CR of -0.125 mpy/c. Our experimental measurement is then verified by using the standard immersion test. The obtained results showed very good consistency in the

measured trends. Moreover, the effect of pH on the CR is also studied by the pH variation of corrosive solutions through adding the distilled water into nitric acid and sodium hydroxide (NaOH). The obtained results showed that the CR is very susceptible to the pH value where for pH of ~ 13 the CR was jumped to ~ 75 mpy. Finally, the performance of the fabricated sensor is demonstrated by CR measurement of the provided water from the Persian Gulf. We received a very good response from the fabricated OTDR-based sensor for field experiment, which confirmed the reliability of the measurements.

References

- [1] SINCHENKO E., *Fibre optic distributed corrosion sensor*, [In] *Centre for Atom Optics and Ultrafast Spectroscopy*, Swinburne University of Technology, 2013.
- [2] SAYING DONG, GANGDING PENG, YANAN LUO, *Preparation techniques of metal clad fibres for corrosion monitoring of steel materials*, *Smart Materials and Structures* **16**(3), 2007, pp. 733–738.
- [3] SAYING DONG, YANBIAO LIAO, QIAN TIAN, *Sensing of corrosion on aluminum surfaces by use of metallic optical fiber*, *Applied Optics* **44**(30), 2005, pp. 6334–6337.
- [4] ROBERGE P.R., *Handbook of Corrosion Engineering*, McGraw-Hill, 1999.
- [5] SAYING DONG, YANBIAO LIAO, QIAN TIAN, YANAN LUO, ZHIGANG QIU, SHIZHE SONG, *Optical and electrochemical measurements for optical fibre corrosion sensing techniques*, *Corrosion Science* **48**(7), 2006, pp. 1746–1756.
- [6] LOPEZ-HIGUERA J.M., RODRIGUEZ COBO L., QUINTELA INCERA A., COBO A., *Fiber optic sensors in structural health monitoring*, *Journal of Lightwave Technology* **29**(4), 2011, pp. 587–608.
- [7] XIAOYI BAO, LIANG CHEN, *Recent progress in distributed fiber optic sensors*, *Sensors* **12**(7), 2012, pp. 8601–8639.
- [8] DYER S.D., TANNER M.G., BAEK B., HADFIELD R.H., SAE WOO NAM, *Analysis of a distributed fiber-optic temperature sensor using single-photon detectors*, *Optics Express* **20**(4), 2012, pp. 3456–3466.
- [9] KURASHIMA T., HORIGUCHI T., TATEDA M., *Distributed-temperature sensing using stimulated Brillouin scattering in optical silica fibers*, *Optics Letters* **15**(18), 1990, pp. 1038–1040.
- [10] TAO WEI, XINWEI LAN, HAI XIAO, YUKUN HAN, HAI-LUNG TSAI, *Optical fiber sensors for high temperature harsh environment sensing*, 2011 IEEE Instrumentation and Measurement Technology Conference (I2MTC), 2011, pp. 1–4.
- [11] TEXIER S., PAMUKCU S., TOULOUSE J., *Advances in subsurface water-content measurement with a distributed Brillouin scattering fibre-optic sensor*, *Proceedings of SPIE* **5855**, 2005, p. 555.
- [12] HENAULT J. M., SALIN J., MOREAU G., DELEPINE-LESOILLE S., BERTAND J., TAILLADE F., QUIERTANT M., BENZARTI K., *Monitoring of concrete structures using OFDR technique*, *AIP Conference Proceedings* **1335**, 2010, p. 1386.
- [13] KAI TAI WAN, C.K.Y. LEUNG, *Durability tests of a fiber optic corrosion sensor*, *Sensors* **12**(3), 2012, pp. 3656–3668.
- [14] YU F.T.S., SHIZHUO YIN, *Distributed fiber optic sensors*, [In] *Fiber Optic Sensors*, CRC Press, 2002.
- [15] THYAGARAJAN K.S., AJOY GHATAK, *Fiber Optic Essentials*, Wiley-IEEE Press, 2007.
- [16] CRISP J., ELLIOTT B., *Introduction to Fiber Optics*, Elsevier, 2005.
- [17] KHORSANDI A., SHOJAEI S., HOSSEINIBALAM F., *Second-harmonic laser-coupled optical fiber sensor for pH measurement and corrosion detection based on evanescent field absorption*, *Optics and Laser Technology* **44**(5), 2012, pp. 1564–1569.
- [18] WANG Y., HUANG H., *Optical fiber corrosion sensor based on laser light reflection*, *Smart Materials and Structures* **20**(8), 2011, article 085003.

- [19] NASCIMENTO J.F., SILVA M.J., COELHO I.J.S., CIPRIANO E., MARTINS-FILHO J.F., *Amplified OTDR systems for multipoint corrosion monitoring*, *Sensors* **12**(3), 2012, pp. 3438–3448.
- [20] MARTINS-FILHO J.F., FONTANA E., *Optical fibre sensor system for multipoint corrosion detection*, [In] *Optical Fiber New Developments*, Lethien C. [Ed.], InTech, 2009.
- [21] BUERCK J., ROTH S., KRAEMER K., MATHIEU H., *OTDR distributed sensing of liquid hydrocarbons using polymer-clad optical fibers*, TDR, 2001.
- [22] MARTINS-FILHO J.F., FONTANA E., GUIMARAES J., PIZZATO D.F., SOUZA COELHO I.J., *Fiber optic based corrosion sensor using OTDR*, 2007 IEEE Sensors, 2007, pp. 1172–1174.
- [23] VARGEL C., *Corrosion of Aluminium*, Elsevier, 2004.
- [24] SZKLARSKA-SMIALOWSKA Z., *Pitting corrosion of aluminum*, *Corrosion Science* **41**(9), 1999, pp. 1743–1767.

*Received April 22, 2015
in revised form September 2, 2015*